Korean J. Chem. Eng., 35(10), 2036-2042 (2018)
DOI: 10.1007/s11814-018-0110-0

pISSN: 0256-1115
eISSN: 1975-7220

Nanoliter scale microloop reactor with rapid mixing ability for biochemical reaction

Seong-Geun Jeong*,‡, Jae-Hoon Jeong,‡, Kyoung-Ku Kang*, Si Hyung Jin*, Byungjin Lee*, Chang-Hyung Choi***,†, and Chang-Soo Lee*,†**

*Department of Chemical Engineering and Applied Chemistry, Chungnam National University, Daejeon 34134, Korea
**Lotte Chemical R&D Center, Daejeon 34110, Korea
***Division of Cosmetic Science and Technology, Daegu Haany University, Gyeongsan 38610, Korea
(*Received 27 April 2018 • accepted 24 June 2018*)

Abstract−The mixing rate is a crucial factor in determining the reaction rate and product distribution in reactors for academic and industrial application. Especially, in pharmaceutical or dangerous chemistry, it is essential to create rapidly homogeneous mixture under the control of a small volume of precious sample. In this study, we propose a microloop reactor that is capable of rapid mixing for homogeneous reaction by utilizing programmable actuated microvalves (PAVs), which can generate the rotary flow rapid mixing in the reactor. The microloop reactor is composed of a stacked layered structure, which is prepared by a soft lithography method. The top layer (fluidic layer) has microchannels for supplying each reagent that is assembled with the bottom layer (control layer). The bottom layer has ultrathin polymer membrane, which can be an on-off valve to precisely control the nanoliter-scale volume of reagents in the reactor. To evaluate mixing performance, we use peroxidase reaction that produces fluorescent by-product (resorufin), thereby observing how fast they are mixed together. We quantify the uniformity of fluorescent intensity throughout the reaction loop, indicating that our proposed microloop reactor exhibits a homogeneous reaction. We envision the microreactor has potential to provide optimized microenvironments in which to perform dangerous chemistry, pharmaceuticals.

Keywords: Microfluidic Reactor, Rapid Mixing, Precise Control of Fluid, Biochemical Reaction, Nanoliter

INTRODUCTION

The mixing rate is a crucial factor in determining the reaction rate and product distribution in reactors [1,2]. Specially, the factor is highly important for a reaction involving extremely unstable intermediates or viscous reaction medium as in polymerization reaction. Thus, in reactor design, it is essential to consider the ability of a reactor to rapidly generate a homogenous reactant mixture after the initial reaction. In traditional chemical reactors, to increase the mixing rate, an impeller (or agitator) is used for mixing reactants. The convection of shear stress induced by an impeller significantly decreases as the distance from reaction container stirrer increases [1,2]. The decrease in convection causes inhomogeneity of the reactant concentrations throughout the container. The local concentration gradients result in unproductive chemistry, increasing reaction times and decreasing efficiency for target products. Thus, the primary technical issue in traditional reactors is to achieve rapid mixing while minimizing the inhomogeneity of reactant in the reactor.

Microfluidic reactors have received substantial attention toward solving their technical issues [1-9]. They provide rapidly homogeneous mixing that leads to faster reactions than those performed by conventional reactors [6,10]. This mixing leads to an increase in selectivity and conversion for synthesis in microfluidic reactors. Thus, microfluidic reactors clearly show high yields compared to those of bulk reactors [1,2]. Continuous-flow synthesis in microfluidic reactors is especially attractive to industry due to such inherent properties as rapid homogeneous mixing [11-14]. However, continuous-flow microfluidic reactors exhibit a lack of control in manipulating small volumes of reactant. Thus, there are still challenges for special reactions that use small volumes of valuable samples, such as with some pharmaceuticals [1,2,15-17]. In addition, it is difficult to control the continuous-flow synthesis of dangerous reactions in micro reactors, such as for explosives or toxic intermediates. A droplet-based microfluidic device enables rapid mixing of multiple reagents in milliseconds by use of oscillating interfacial shear from protrusions of the microchannel walls within the drops [18-20]. However, this system has difficulty in scaling up the proposed microloop design because it is hard to merge two droplets for mixing multiple reagents. This problem becomes significant when several droplets are required to merge with each other for rapid mixing of multiple reagents at the same time. In addition, this system has critical problems such as contamination, synchronization, precise control of concentration in droplet [18,21,22]. Taken together, with these aspects present, the system has difficulty in scaling up the proposed microloop design.

Microfluidic Loop reactors provide rapid mixing of multiple reagents and precise control of small volumes in a simple, efficient and programmable manner. Hansen et al. demonstrated the loop reactor for rapidly generating complex mixtures in nanoliter scale reactor, which is applied to systematically study the phase behavior of the protein exylanase over a large and complex chemical space

†To whom correspondence should be addressed.
E-mail: rhadum@cnu.ac.kr, cchoi@dhu.ac.kr
‡These authors contributed equally to this work.

[23]. Ridgeway et al. showed the loop reactor facilitates the study of kinetics of RNA-protein complex formation over long time scales [24]. Kim et al. demonstrated rapid sampling of biomolecule conformational landscape and of enzymatic activity in their loop reactor [25]. Although many types of loop reactors have been reported to study biological research, they have not been applied to peroxidase reaction using hydrogen peroxide that can be released from biological samples in research applications. In addition, the initial reaction rate for peroxides reaction is not yet reported in the nanoliter-scale loop reactor.

Here, we performed a peroxidase reaction in the loop reactor to study experimental condition for biochemical reaction in microfluidic system. The loop reactor provides rapid mixing with programmable actuated microvalves (PAVs) that can create homogeneous mixing using nanoliter-scale volumes as reagents. This system provides the fluorescence-based measurement of reaction rate as function of reactants.

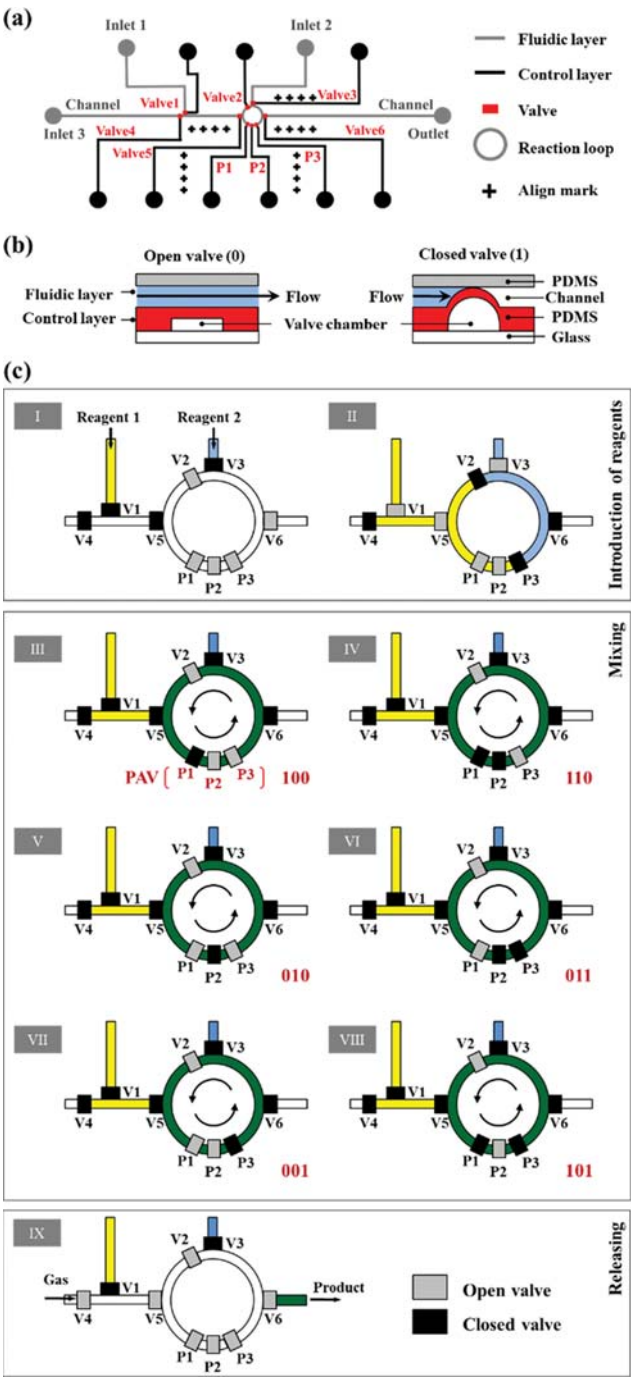

Fig. 1. The basic concept of a microloop reactor for rapid mixing. (a) The microloop reactor consists of fluidic and control layers. The fluidic layer contains channels, Inlet 1, Inlet 2, Inlet 3 and an outlet (gray line and circle). Inlet 1 and Inlet 2 were used to inject reagents. Inlet 3 was used to inject nitrogen gas to release the product from the reaction loop to the outlet. The control layer (black line and circle) contains micro valves (from valve 1 to valve 6) and programmable actuated valves (P1, P2, and P3, in red). Valve 6 controls the injection and transfer of reagents and gas in the fluidic channel. The programmable actuated valve (PAVs) generates rotary flow to mix reagents rapidly and homogeneously in the reaction loop. (b) The principle of operation for opening and closing the valve is as follows. The closed valve is expanded, which enables the stopping of fluid flow in the fluidic channel. The opened valve is not expanded, which allows fluid flow into the fluidic channel. The process of fully mixing reagents 1 and 2 in the reaction loop by PAVs comprises the following steps: injection (I-II), mixing (III) and releasing (IV). (c) The diagram of operation for a reaction in the loop reactor. Introduction of reagents into the loop reactor when valve 1 and valve 3 are open (from I to II). Rotary mixing when the PAVs operates according to a preprogrammed sequence, as 100-110-010-011-011-101 (from III to VIII). This sequence of the PAVs generates rotary flow for rapid mixing in the reaction loop. Nitrogen gas is injected to release the product from the reactor to the outlet (IX). Gray and black boxes indicate opened and closed valves, respectively.

EXPERIMENTAL

1. Design of Microloop Reactor

The microfluidic loop reactor was designed by AutoCAD software (Autodesk, Inc., USA). Fig. 1(a) shows the configuration of PAVs in the microloop reactor. The designed microfluidic reactor consists of fluidic and control channel layer. First, the fluidic channel layer includes three inlets for injection of two reagents and nitrogen gas, one outlet and loop reactor. All designed channels have 100 μm width and 15 μm height. The inner diameter and the maximum fluorescence in volume of the loop reactor is 1 mm and 0.47 nL, respectively. Second, the control channel layer includes six valves and PAVs. PAVs consist of P1, P2 and P3 valve (Fig. 1(c)). The six valves enable one to control the fluid toward the loop reactor and outlet. PAVs are to generate rotary flow in the loop reactor. Both two layers have align marks in order to stack layers vertically as designed during soft lithography.

2. Fabrication of Microfluidic Loop Reactor

The reactor was fabricated by using photolithography and soft lithography [6,7,26-31]. First, a micromold of the fluidic layer was fabricated using AZ9260 positive photoresist (MicroChem, MA, USA) on a silicon wafer. The photoresist was spin-coated on the silicon wafer and then exposed to visible light [32,33]. The wafer

was developed with AZ 400 K (MicroChem, MA, USA) to form a fluidic channel pattern with a 15 μm height. Polydimethylsiloxane (PDMS, Dow Corning, MI, USA) and a curing agent were prepared by mixing and degassing in a vacuum chamber. The degassed PDMS was poured onto the silicon master and partially cured at 65 °C in an oven for 1 hr. Second, the micromold of the control layer was fabricated using SU-8 3025 negative photoresists (MicroChem, MA, USA) to form a control layer pattern with a height of 15 μm. The degassed PDMS was poured onto the silicon wafer and partially cured at 65 °C in an oven for 45 min. The PDMS of the control layer was then detached from the wafer. Third, the partially cured PDMS of the fluidic layer was aligned and assembled on the partially cured PDMS of the control layer using the alignment marks. The assembled PDMS was fully cured for 6 hr at 65 °C. The fully cured PDMS was punched to form holes to connect the inlet to the fluidic and control channels. Finally, the punched PDMS and the glass substrate were bonded under oxygen plasma (PDC-002, Harrick, USA) for 2 min.

3. Operation of the Microloop Reactor for Biochemical Reactions

Microfluidic operation is based on using a valve to control fluid flow in the fluidic channel [34]. The opening and closing of all the valves are controlled by using a pneumatic valve by applying positive pressure with nitrogen gas. The pressure for valves in the fluidic channel was controlled with an air compressor (GAST P104-AA, IDEX Corp. USA), which can also adjust the flow rate in the fluidic channels. For the valve, the pressure determines the open/close status of the valve (Fig. 1(b)). When the nitrogen gas is injected into the microchannel of the valve, the valve chamber is expanded and the fluid microchannel is closed. In the opposite case, when the nitrogen gas is not injected into the microchannel of the valve, the valve chamber is not expanded, and the fluid microchannel remains open.

Based on this concept, we controlled the injection and reaction of reagents in the reactor (Fig. 1(c)). First, 10 mM hydrogen peroxide (Sigma-Aldrich, MO, USA) (reagent 1) was injected through inlet 1 while valve 1, valve 4 and valve 5 were closed (I in Fig. 1(c)). Second, a mixture (reagent 2) of 0.1 to 1 mM Amplex Red (Sigma-Aldrich, MO, USA) and 2 U/ml horseradish peroxide (HRP) (Sigma-Aldrich, MO, USA) was injected through inlet 2 while valve 3 was closed (I in Fig. 1(c)). Third, two reactants were introduced to the loop reactor while only valve 1, valve 3, valve 5, P1 and P2 were open (II in Fig. 1(c)). Valves 2 and P2 prevent mixing of the two reagents before the desired start time. Fourth, the PAVs generate rotary flow to mix the two reagents rapidly for a homogeneous reaction in the reactor when valve 2 opens, and then valve 1, valve 3, valve 4, valve 5 and valve 6 are closed (III-VIII in Fig. 1(c)). The PAVs operates according to a programmed sequence as 100-110-010-011-110-101 for the generation of rotary flow. In the sequence, '1' and '0' indicate the opened and closed valve, respectively. The circular sequence of the PAVs can generate flow vibrations in the fluid in the microloop channel, and this can generate rotary flow. The circular sequence speed is 6 Hz, and this is enough to generate rotary flow [10]. Valve 3, valve 5 and valve 6 each prevent the leak of reagents out of the reactor during the mixing process. Fifth, nitrogen gas is introduced through inlet 3 when only valve 1 and valve 3 are closed (IX in Fig. 1(c)). The product is released from the loop reactor outlet when V6 opens the channel to the outlet.

4. The Optimization of PAVs Condition for Rapid Mixing in Microreactor

We prepare a microfluidic device as we integrate the PAVs into the loop reactor (Fig. 1). The PAVs generate rotary flow in the loop reactor. In our previous work, we confirmed optimization condition for rapid in the loop reactor by measuring the gray intensity of mixture during mixing of water and food dye [10]. First, the intensity of gray value of the mixture was measured at different pressure from 0.3 to 0.5 MPa, which is applied to valves in the reactors. The intensity reaches the maximum value at 0.4 and 0.5 MPs after about 5 and 6 second, respectively; the maximum value indicates full mixing of reagents. Although fast mixing occurs under strong pressure conditions (0.5 MPs), the shape of channel is deformed due to the strong pressure. In the case of 0.3 MPs, the intensity dose not reach to the maximum value within 10 s. Therefore, we selected the optimization condition of pressure for rapid mixing as 0.4 MPs without critical issue about the deformation of channel. Second, the intensity of gray value is measured at different frequency from 2 to 12 Hz. Although the intensity does not reach the maximum value within 10 s at 2 and 4 Hz, the intensity reaches the maximum value within 8 s at higher than 4 Hz. Therefore, we conclude the optimization condition for rapid and fully mixing is 0.4 MPs and 6 Hz.

5. Analytical Method for Evaluating the Chemical Reaction

The mixing performance of two reagents was analyzed using a microscope and image program. First, an inverted fluorescence microscope (TE2000, Nikon, Japan) filter set (Nikon Texas Red; excitation wavelength 540-580 nm, emission wavelength 600-660 nm) and a CCD camera (Collapse cf, Photometrics, USA) was used to take images at specific regions of the loop reactor. Second, the images were analyzed by ImageJ and Image-Pro (Media Cybernetics, USA). The full mixing time of the two reagents was calculated by measuring the mean gray value at the specific area in the reaction loop reactor that involved the mixture of reagents. The criterion to determine the full mixing time is the value when the fluorescence intensity reaches the saturation point.

RESULTS AND DISCUSSION

1. Evaluation of Rapid Mixing Efficiency

Here, we demonstrate that rapid mixing can be achieved by utilizing a microloop reactor. To validate this, we used a model biochemical reaction with Amplex Red, HRP and H_2O_2. Specifically, Amplex Red is oxidized by H_2O_2 in the presence of HRP and converted to a fluorescent by-product (resorufin) [35-37], which has an emission and excitation wavelength of 585 and 571 nm, respectively (Fig. 2(a)), implying that we can simply observe how fast the reaction proceeds in the reaction loop. Both reactants for the reaction were sequentially injected into the microloop reactor through inlets 1 and 2 (Fig. 1(c)). The reaction was carried out through mixing in the microloop channel with two streams, which consisted of 5 μM H_2O_2 (reagent 1) and a mixture of 0.1 mM Amplex Red and 0.2 U/ml HRP (reagent 2). The frequency of PAVs operations and the applied pressure of the PAVs to mix and react the two reagents are 6 Hz and 0.4 MPa, respectively. Upon initial operation of the

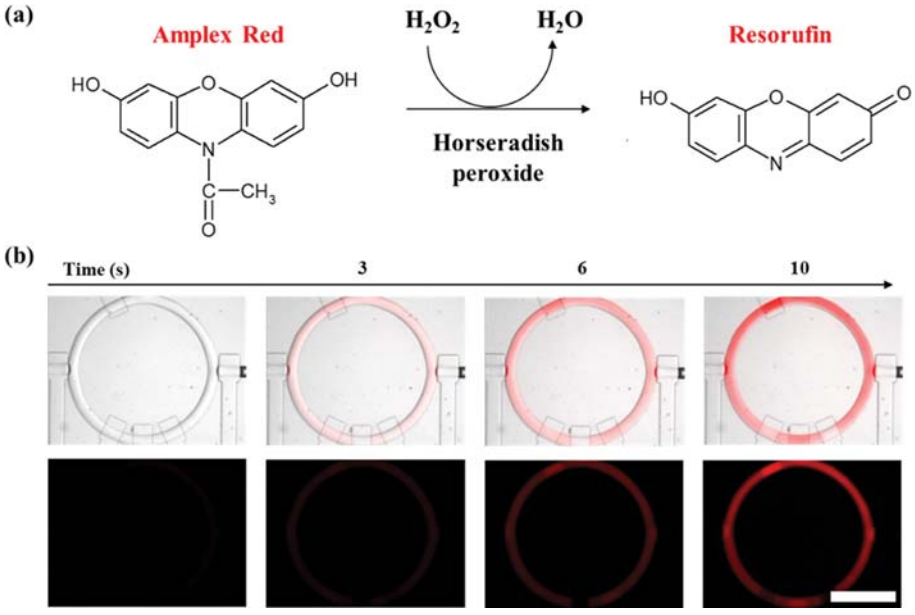

Fig. 2. Evaluation of rapid mixing efficiency of the loop reactor using a biochemical model reaction. (a) Model biochemical reaction: Conversion of Amplex Red into Resorufin. Horseradish peroxidase (HRP) uses Amplex Red as an electron donor during the reduction of hydrogen peroxide to water; (b) Fluorescence (bottom) and composite images (top) showing conversion of Amplex Red into Resorufin as a function of time. The scale bar indicates 500 μm.

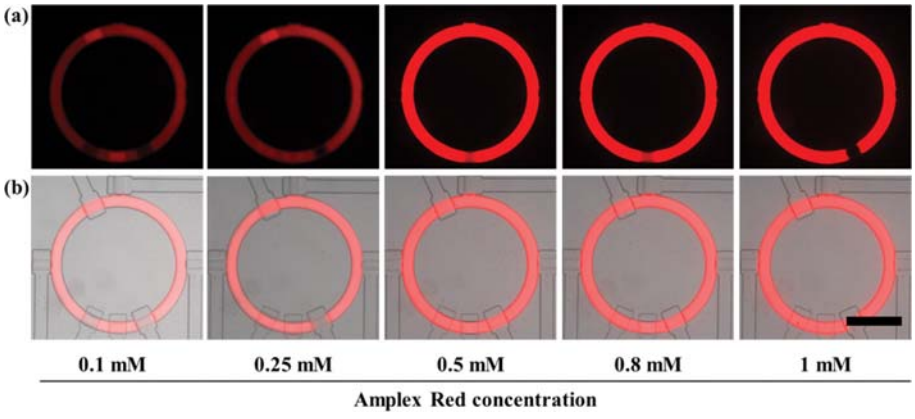

Fig. 3. The effect of Amplex Red concentration on the homogeneous mixing. Fluorescence (a) and composite (b) images showing fluorescent intensity in each reactor with varying initial concentration of Amplex Red. All the images were captured immediately after we operated the microreactor for 10 sec. The scale bar indicates 500 μm.

PAVs, the fluorescence signal was not observed, while the signal was clearly observed at 10 s as the resorufin was produced, as seen in the fluorescence and composite images of Fig. 2(b). This result indicates that the PAVs integrated microloop reactor provides sequential injection of multiple reagents in a precisely controlled manner. Furthermore, we achieved rapid mixing of the supplied reagents in a simple and programmable manner.

2. Evaluation of the Homogeneous Mixing

We further investigated the effect of Amplex Red concentration on homogeneous mixing efficiency in the microreactor. For this, we varied the concentration of Amplex Red from 0.1 to 1 mM at a fixed concentration of HRP. The reactors at different reagent conditions were imaged after 10 s (reaction time) via fluorescence microscopy, as shown in Fig. 3. Upon rapid mixing, the maximum fluorescence intensity increased as the initial concentration of Amplex Red increased because the amount of by-product converted (resorufin) depends on the concentration of Amplex Red. Importantly, although fluorescent intensity varied, uniformity of the intensity profile in each reaction loop (condition) was consistent, indicating that the initial reaction concentration of Amplex Red did not affect the homogeneous mixing efficiency of the reactants. The maximum fluorescence intensity with initial reactant concentration was similar after 0.5 mM Amplex Red. This indicates that the reaction was terminated and that the biochemical reaction, which is the model reaction used in this study, is a 1 : 1 equivalent reaction as shown in Fig. 2(a). When the concentration of the initial reactant exceeds the number of reaction equivalents, the concentration of the product cannot exceed the chemical reaction equivalent. The result is

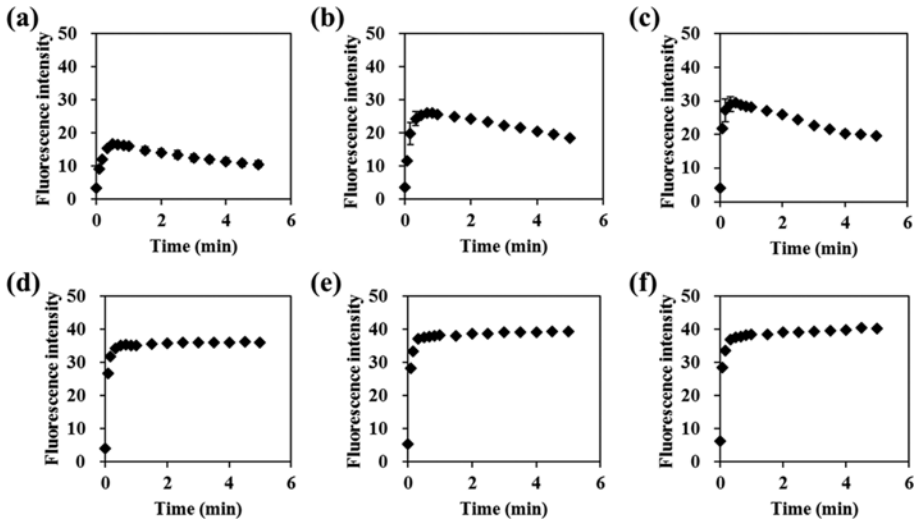

Fig. 4. Quantitative analysis of a biochemical reaction and fluorescence intensity as function of time and Amplex Red concentration: (a) 0.1 mM, (b) 0.25 mM, (c) 0.4 mM, (d) 1 mM, (e) 1.5 mM and (f) 2 mM. The maximum fluorescence intensity was reached in approximatively 10 s in the reaction loop. The microloop reactor is exposed to visible light when the fluorescence intensity is measured.

indirect evidence of the reaction mechanism, depending on the concentration of the reactants. So, if the concentration of the reactant can be finely controlled, then this reactor can be used to indirectly predict the maximum conversion rate, depending on the mechanism of the chemical reaction and the reaction conditions.

3. Quantitative Analysis of Biochemical Reaction

The change in fluorescence intensity depending on the reaction time under various initial concentrations of Amplex Red is quantitatively presented in Fig. 4. Although there were slight differences depending on the initial concentration of Amplex Red, one can see that the maximum fluorescence intensity occurs within approximately 10 s. This implies that each reaction can be completely terminated in under 10 s. Interestingly, when the initial concentration of Amplex Red is in the low range of 0.1 mM to 0.4 mM, the fluorescence intensity gradually decreases over the reaction time, after reaching the maximum fluorescence intensity. These results originate from the decomposition of resorufin, which can be damaged by visible light [38]. With real-time fluorescence intensity monitoring, the microloop reactor is exposed to visible light (540-580 nm). Long-term exposure to visible light can decompose the converted resorufin, thereby decreasing the fluorescence intensity. However, at higher concentrations of Amplex Red (1 mM to 2 mM), the fluorescence intensity is maintained or slightly increased after reaching the maximum fluorescence intensity. These results can be explained by the formation of new resorufin, which comes from the photooxidation of residual unreacted Amplex Red. When the initial concentration of Amplex Red is higher than the equivalence of the chemical reaction balance, there will be an excess of Amplex Red, and as the reaction progresses, hydrogen peroxide will be mostly consumed by the reaction. Thus, a significant amount of excess Amplex Red remained in the reactor, as unreacted. This residual unreacted Amplex Red cannot be converted into resorufin without hydrogen peroxide. The resorufin can be decomposed by visible light, and this causes a decrease in the fluorescence intensity. However, the opposite phenomenon can be induced by visible light. That is, photooxidation of Amplex Red can produce resorufin [38, 39]. Although the resorufin is decomposed, the Amplex Red can be converted to resorufin by photooxidation when the microloop reactor contains residual unreacted Amplex Red. These two reactions can occur simultaneously in one reactor and the decomposition and generation of each component can be approximately in equilibrium. We conclude that these results are due to these two opposite reactions.

The reaction of Amplex Red is a chemical reaction with the equivalent ratio shown in Fig. 2(a). Ideally, when the reaction is carried out, the minimum amount of introduced reactant determines the total amount of the final product. The experimental results were carried out under fixed reaction conditions except for the initial concentration of Amplex Red (Fig. 4). The reaction results showed that the addition of an excess amount of Amplex Red could be distinguished, and additional changes in the residual unreacted material could be observed depending on the reaction equivalent ratio. These sensitive and precise reaction results show that the microloop reactor integrated with PAVs can have a significant level of sensitivity. These results may be indirect evidence of the precision of the microloop reactor.

In addition, we obtained the slope of fluorescence intensity for resorufin (Fig. 5(a)) from the fluorescence intensity data (Fig. 4) within 10 s as a function of Amplex Red. The slope of the fluorescence of resorufin is determined by the reaction rate of Amplex Red within 10 s after injection and mixing of the reagents (Fig. 5(b)). The slopes can be converted to the reaction rate. Thus, the reaction rate is defined as the concentration of resorufin per unit time (mM/s). We obtained the reaction rate by using use the calibration curve of fluorescence intensity of resorufin (inset of Fig. 5(a)). The resulting uncertainty in the determinations of the reaction rate is due to time deviation that is shown in the error bars in Fig. 5(a) and (b). Although, at a higher concentration (>1 mM), the slope and reaction rate are not significantly changed because excess Amplex Red cannot be converted, due to a lack of hydrogen peroxide in the ini-

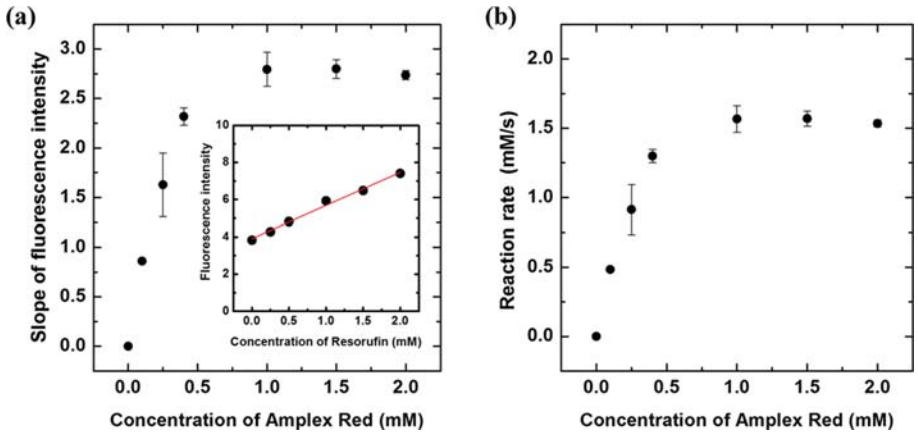

Fig. 5. Production rate of resorufin. (a) A plot showing fluorescence intensity of resorufin as a function of the Amplex Red concentration. (Inset) Calibration curve for relation between fluorescence intensity and concentration of resorufin. (b) Reaction rate as a function of Amplex Red concentration.

tial reaction state. At a lower concentration (<1 mM), the initial reaction rate and the slope of fluorescence intensity increases as a function of the Amplex Red concentration. This result clearly shows the reaction rate can be controlled in the loop reactor by adjusting the initial concentration of Amplex Red.

Finally, we compared the diffusion-based mixing time and our PAVs-based mixing time to prove that PAVs-based mixing is rapid than diffusive process. In general microfluidic systems, the mixing efficiency is very low because chemical reactions are dominated by diffusion at an interface because the system operates at low Reynolds numbers ($<10^2$) and generates laminar flow [45]. First, to compare the type of mixings, we obtained diffusion coefficient of HRP using stoke-Einstein equation as follows [46]:

$$D = \frac{k_B T}{6\pi\eta r}$$

Here, D is diffusion coefficient. η and r are viscosity of fluid and radius of particle. k_B is Boltzmann constant as 1.38×10^{-23} m^2 $kg/s^2\cdot K$. T is temperature of fluid. Stokes radius of horseradish peroxidase (HRP) is 3.0 nm [47]. When T and η are 293.15 K and 1.0016 m·Pa·s, diffusion coefficient (D) of HRP is 71.45 $\mu m^2/s$. In our microfluidic system, area of microLoop channel (A) is 3.46×10^5 μm^2. After introduction of two reagents, the two fluids fill half of the reactor. The approximate mixing time (t_m) is t_m=0.5 A/D. Thus, mixing time is 2.43×10^3 seconds. However, our fluorescence-based analysis presents the mixing as complete in 10 s. It is strong evidence that the PAV-based mixing is clearly achieved in convection-dominated regime where it is overwhelmingly more rapid than a diffusive process.

CONCLUSION

We have demonstrated a great mixing capability to peroxidase reaction by utilizing PAVs integrated microloop reactor. This chemical reaction is achieved by sequential loading of H_2O_2, HRP and Amplex red through the separate microchannel, and they are subsequently mixed together within the microreactor under optimized operation condition of PAVs in the microloop reactor. Importantly, this microloop reactor enables fluorescence-based real-time monitoring of products (resorufin) synthesized under rapid mixing of reagents; this system could be beneficial for drug screening that must handle tiny volume of expensive biochemicals. We find the fluorescence intensity is determined by concentration of the products upon the reaction; this enables us to estimate reaction rate based on quantitative analysis of varying fluorescence signal. In addition, the fluorescence-based real-time monitoring of resorufin produced by peroxidase reaction in microfluidic system can be used for H_2O_2 assay, because the amount of the resorufin is equivalent to consumed H_2O_2 in the peroxidase reaction (Fig. 2(a)). Furthermore, the H_2O_2 assay is important in cellular physiology because H_2O_2 is a non-radical oxidant present in organisms; its cellular function plays a key role in cellular signals [48]. Overall, our proposed microloop reactor can provide a great platform for optimizing chemical reaction conditions for both research and industrial applications [40-44].

ACKNOWLEDGEMENTS

This work is supported by Global Research Laboratory ICT (NRF-2015K1A1A2033054) through the National Research Foundation of Korea (NRF) funded by the Ministry of Science and ICT (Information and Communication Technologies).

REFERENCES

1. A. J. deMello, *Nature*, **442**, 394 (2006).
2. K. S. Elvira, X. Casadevall i Solvas, R. C. Wootton and A. J. deMello, *Nat. Chem.*, **5**, 905 (2013).
3. C. C. Lee, G. Sui, A. Elizarov, C. J. Shu, Y. S. Shin, A. N. Dooley, J. Huang, A. Daridon, P. Wyatt, D. Stout, H. C. Kolb, O. N. Witte, N. Satyamurthy, J. R. Heath, M. E. Phelps, S. R. Quake and H. R. Tseng, *Science*, **310**, 1793 (2005).
4. I. Jang and S. Song, *Lab. Chip*, **15**, 3405 (2015).
5. K. Y. Ko and I. H. Kim, *Biotechnol. Bioprocess Eng.*, **21**, 453 (2016).
6. H. H. Jeong, D. Issadore and D. Lee, *Korean J. Chem. Eng.*, **33**, 1757 (2016).
7. R. Singh, H. J. Lee, A. K. Singh and D. P. Kim, *Korean J. Chem. Eng.*,

33, 2253 (2016).
8. S. Andarwa and H. B. Tabrizi, *Korean J. Chem. Eng.*, **34**, 1319 (2017).
9. J. J. Zhong, *Korean J. Chem. Eng.*, **27**, 1035 (2010).
10. S. H. Jin, J.-H. Jung, S.-G. Jeong, J. Kim, T. J. Park and C.-S. Lee, *Front. Chem. Sci. Eng.*, **12**, 239 (2017).
11. N. Kockmann, M. Gottsponer, B. Zimmermann and D. M. Roberge, *Chemistry-a European J.*, **14**, 7470 (2008).
12. M. Rahimi, P. Valeh-e-Sheyda and H. Rashidi, *Korean J. Chem. Eng.*, **34**, 3017 (2017).
13. J. J. Sim, H. J. Moon, Y. H. Roh, H. W. Jung and K. W. Bong, *Korean J. Chem. Eng.*, **34**, 1495 (2017).
14. T. H. Tran, W. J. Chang, Y. B. Kim, Y. M. Koo, E. K. Kim, J. Y. Yoon and J. Kim, *Biotechnol. Bioprocess Eng.*, **12**, 470 (2007).
15. G. M. Whitesides, *Nature*, **442**, 368 (2006).
16. L. F. Kang, B. G. Chung, R. Langer and A. Khademhosseini, *Drug Discovery Today*, **13**, 1 (2008).
17. S. G. You and S. J. Bai, *Biotechnol. Bioprocess Eng.*, **22**, 474 (2017).
18. A. Liau, R. Karnik, A. Majumdar and J. H. D. Cate, *Anal. Chem.*, **77**, 7618 (2005).
19. C. L. Grigsby, Y. P. Ho, C. Lin, J. F. J. Engbersen and K. W. Leong, *Scientific Reports*, **3**, 3155 (2013).
20. C. Y. Lee, C. L. Chang, Y. N. Wang and L. M. Fu, *Int. J. Mol. Sci.*, **12**, 3263 (2011).
21. Z. Y. Zhang, P. Zhao, G. Z. Xiao, M. Lin and X. D. Cao, *Biomicrofluidics*, **2**, 014101 (2018).
22. K.-K. Kang and C.-S. Lee, *ACS Central Sci.*, **4**, 434 (2018).
23. C. L. Hansen, M. O. A. Sommer and S. R. Quake, *Proceedings of the National Academy of Sciences of the United States of America*, **101**, 14431 (2004).
24. W. K. Ridgeway, E. Seitaridou, R. Phillips and J. R. Williamson, *Nucleic Acids Res.*, **37**, 142 (2009).
25. S. Kim, A. M. Streets, R. R. Lin, S. R. Quake, S. Weiss and D. S. Majumdar, *Nature Methods*, **8**, 242 (2011).
26. S. H. Jin, S. S. Lee, B. Lee, S. G. Jeong, M. Peter and C. S. Lee, *Anal. Chem.*, **89**, 9722 (2017).
27. S. H. Jin, S. C. Jang, B. Lee, H. H. Jeong, S. G. Jeong, S. S. Lee, K. P. Kim and C. S. Lee, *Lab on a Chip*, **16**, 1358 (2016).
28. H. H. Jeong, B. Lee, S. H. Jin, S. G. Jeong and C. S. Lee, *Lab on a Chip*, **16**, 1698 (2016).
29. H. H. Jeong, S. H. Jin, B. J. Lee, T. Kim and C. S. Lee, *Lab on a Chip*, **15**, 889 (2015).
30. M. Su, *Korean J. Chem. Eng.*, **34**, 484 (2017).
31. S. Jung and H. Yi, *Korean J. Chem. Eng.*, **32**, 1713 (2015).
32. S. Jung, Y. Tang, G. Shim, C.-S. Lee, C.-H. Choi and H. Yi, *Biochem. Eng. J.*, **135**, 123 (2018).
33. J. Kim, S. H. Jin, K.-K. Kang, Y.-M. Chung and C.-S. Lee, *Chem. Eng. Sci.*, **175**, 168 (2018).
34. M. A. Unger, H. P. Chou, T. Thorsen, A. Scherer and S. R. Quake, *Science*, **288**, 113 (2000).
35. J. W. Hong, V. Studer, G. Hang, W. F. Anderson and S. R. Quake, *Nature Biotechnol.*, **22**, 435 (2004).
36. M. J. Zhou, Z. J. Diwu, N. PanchukVoloshina and R. P. Haugland, *Anal. Biochem.*, **253**, 162 (1997).
37. M. Razzaghi, A. Karimi, H. Aghdasinia and M.-T. Joghataei, *Korean J. Chem. Eng.*, **34**, 2870 (2017).
38. S. Miwa, A. Treumann, A. Bell, G. Vistoli, G. Nelson, S. Hay and T. von Zglinicki, *Free Radical Biology and Medicine*, **90**, 173 (2016).
39. B. Z. Zhao, F. A. Summers and R. P. Mason, *Free Radical Biol. Med.*, **53**, 1080 (2012).
40. Y. Jo, K. Kim and J. Choi, *Biotechnol. Bioprocess Eng.*, **21**, 191 (2016).
41. Y. G. Shen, Z. Y. Song, Y. M. Yan, Y. X. Song, X. X. Pan and Q. Wang, *Micromachines*, **8**, 172 (2017).
42. N. T. Nguyen, M. Hejazian, C. H. Ooi and N. Kashaninejad, *Micromachines*, **8**, 186 (2017).
43. K. I. A. Ieong, C. P. Yang, C. T. Wong, A. C. Shui, T. T. Y. Wu, T. H. Chen and R. H. W. Lam, *Micromachines*, **8**, 167 (2017).
44. K.-K. Kang and H.-K. Rhee, *Micropor. Mesopor. Mater.*, **257**, 202 (2018).
45. K. S. Elvira, X. C. i Solvas and R. C. Wootton, *Nat. Chem.*, **5**, 905 (2013).
46. A. Einstein, Investigations on the theory of the Brownian movement, Dover Publications, New York (1956).
47. B. Fu, F. R. Curry, R. H. Adamson and S. Weinbaum, *Ann. Biomed. Eng.*, **25**, 375 (1997).
48. F. Antunes and P. M. Brito, *Redox Biol.*, **13**, 1 (2017).